nature synthesis

Supplementary information

https://doi.org/10.1038/s44160-026-01161-x

Electrosynthesis of arylglycines from carbon dioxide, nitrite and aldehydes

In the format provided by the authors and unedited

Table of Contents

Supplementary Methods

Materials

All reagents were used as received without further purification. K_2HPO_4 (98%), KH_2PO_4 (>99%), KNO_2 (97%), $NaClO_4$ (99%), $KClO_4$ (99%), ferrocene (Fc, 98%), and acetophenone (98%) were purchased from Acros Organics. NH_2OH (50% aqueous solution), *N*,*N*-dimethylformamide (DMF, anhydrous, amine-free, 99.9%), tetrabutylammonium iodide (TBAI, 98%), benzaldehyde (>99%), trisodium citrate dihydrate (99%), perchloric acid (60~62%), $MgCl_2$ (99%), and acetonitrile (99.8%) were purchased from Alfa Aesar. Benzaldoxime (95%) was purchased from Apollo Scientific. Dichloromethane (99.5%) was purchased from BDH Chemicals. Tetrabutylammonium perchlorate (TBAP, >99%), 2-methylbutyraldehyde (95%), $Pb(ClO_4)_2 \cdot 3H_2O$ (98%), zinc trifluoromethanesulfonate ($Zn(OTf)_2$, 98%), and phenylglycine (95%) were purchased from Sigma-Aldrich. Pb foil (99.8%) was purchased from Thermo Scientific. High-purity Ar (99.999%) and NH_3 (10% in Ar) gases were purchased from Airgas. Cyclohexanone was purchased from TCI. 2-Bromo-2-phenylacetic acid, thiophene-2-carboxaldehyde (99.56%), pyrazine-2-carboxaldehyde (98.89%), oxazole-5-carboxaldehyde (97.07%), benzothiophene-2-carboxaldehyde (98%), and quinoxaline-2-carboxaldehyde (99%) were purchased from AmBeed. Hydrochloric acid (99.99%) was purchased from Honeywell. D_2O (99.9%), Zn foil (99.994%), Mg foil (99.9%), Ti foil (99.4%), Cu foil (99.8%), furan-2-carboxaldehyde (99%), butylated hydroxytoluene (BHT, 99%), and pyridine-2-carboxaldehyde (99%) were purchased from Fisher Scientific. Li foil (99.9%) was purchased from MSE Supplies. $AlCl_3$ (99%) was purchased from Strem. Boron-doped diamond electrode (BDD, on a silicon substrate) was purchased from XLeboer. Pt foil electrode was purchased from CH Instruments. Graphite plate (99.9%) was purchased from OTOOLWORLD. Ni foil (99.5%) was purchased from Thomas Scientific. Al foil was purchased from Avantor. Indole-2-carboxaldehyde (99.75%) was purchased from MedChemExpress. **Safety statement:** All experiments involving NH_2OH, perchloric acid, perchlorate salts, Li metal, NH_3, and volatile organic solvents were carried out in a fume hood using appropriate personal protective equipment. NH_2OH and perchlorate-containing materials were handled with appropriate precautions. Li metal was handled under an inert atmosphere. NH_3 was handled with suitable gas containment. All reagents were handled in accordance with their safety data sheets and institutional procedures.

Electrode preparation

Pd electrodes were prepared by sputter-coating a 50 nm film of Pd (99.99%, Rave Scientific) onto Teflon-treated carbon fiber paper (Toray 030, Fuel Cell Store) using a Leica ACE 600 Sputter Coater. The thickness of the deposited metal layer was monitored and controlled using a quartz crystal. Pb/Ni foam electrodes were prepared by electrodeposition. Specifically, Ni foam was first immersed in 1.0 M HCl for 30 min, followed by thorough rinsing with deionized water and acetone. An aqueous electrolyte containing 0.01 M $Pb(ClO_4)_2$, 0.01 M trisodium citrate, and 1 M $HClO_4$ was then prepared and purged with Ar for 30 min to remove dissolved O_2. A Pt plate (1.5 × 1.5 cm^2) was used as the anode, and a piece of Ni foam (1 × 2 cm^2 geometric area) was employed as the cathode, with an interelectrode distance of 2 cm. Electrodeposition was carried out by applying 2.6 V for 30 s, followed by 2.2 V for 30 min. After deposition, the obtained electrode was rinsed thoroughly with acetone and dried.

Electrochemical reduction of nitrite and formation of benzaldoxime

The electrochemical tests were carried out in an H-cell. The cathode chamber contained the working electrode and a Ag/AgCl reference electrode (saturated KCl, Pine Research Instrumentation) placed close to it. A graphite rod served as the counter electrode in the anode chamber. The two chambers were separated by an anion-exchange membrane (Selemion DSV). Each compartment held 12 mL of electrolyte. Prior to each measurement, the electrolyte was pre-saturated with Ar by bubbling the gas at a flow rate of 20 sccm for at least 15 min. Ar gas was continuously bubbled into the electrolyte during electrolysis. Before the start of each electrolysis, the resistance between the reference electrode and the working electrode was determined using potentiostatic electrochemical impedance spectroscopy. The working electrode potential was set to −0.5 V vs Ag/AgCl and the frequency was scanned from 200 kHz to 1 Hz with an amplitude of 10 mV. In the Nyquist plot, the ohmic resistance was determined from the intersection of the measured impedance data with the x-axis. Then, 100% iR compensation was applied to the measurement. For nitrite electroreduction, electrolysis was performed in 0.10 M phosphate buffer (pH 7) containing 0.10 M KNO_2. A Pd electrode (4 × 2 cm^2, 3 × 2 cm^2 immersed) served as the working electrode. The standard condition was −0.1 V vs RHE. All potentials were converted to the reversible hydrogen electrode (RHE) scale using the following formula: V (vs RHE) = V (vs Ag/AgCl) + 0.1976 V + 0.0592 V × pH. Two different procedures were used to couple nitrite reduction with benzaldehyde (Routes S1 and S2). In Route S1, pure benzaldehyde was added to the aforementioned nitrite-containing electrolyte to give a starting concentration of 15 mM before electrolysis, and electroreduction was then performed at −0.1 V vs RHE till the total passed charge reached 20 mAh. In Route S2, nitrite was first electrochemically reduced under the aforementioned conditions. After electrolysis, pure benzaldehyde was added to the electrolyte to give an initial concentration of 15 mM (before reacting with NH_2OH). The 12 mL resulting solution after oxime formation was extracted with 2 mL of dichloromethane three times. The combined organic phase was subsequently evaporated under ambient conditions to obtain the solid product, which was then re-dissolved in 12 mL of DMF to yield a benzaldoxime solution for the next electrochemical carboxylation step. The products were quantified before and after extraction. Specifically, 450 μL of the aqueous electrolyte solution after electrolysis was mixed with 50 μL of D_2O containing 0.01 M MeCN as an internal standard and analyzed by ^1H NMR. After extraction, 100 μL of the resulting DMF solution was diluted with water to a volume of 1 mL, and 450 μL of this new solution was then mixed with 50 μL of D_2O containing 0.01 M MeCN as an internal standard and analyzed by ^1H NMR.

Electroreductive carboxylation of oximes

Heteroaryl aldoximes were prepared directly from the corresponding heteroaryl aldehydes (including furan-2-carboxaldehyde, thiophene-2-carboxaldehyde, pyridine-2-carboxaldehyde, pyrazine-2-carboxaldehyde, oxazole-5-carboxaldehyde, benzothiophene-2-carboxaldehyde, quinoxaline-2-carboxaldehyde, and indole-2-carboxaldehyde) and NH_2OH. Specifically, 5 mL of a 0.5 M aqueous solution or suspension of the heteroaryl aldehyde was prepared, followed by the addition of 1.2 equivalents of NH_2OH (from a 50 wt.% NH_2OH aqueous solution). After thorough mixing and complete reaction, the resulting mixture was frozen in liquid nitrogen and subsequently dried under vacuum to afford the corresponding heteroaryl aldoxime as a solid product. Commercial benzaldoxime was used in reaction condition optimization and mechanistic study experiments (data related to Figs. 3 and 5). Oxime carboxylation was typically carried out in a two-electrode single-cell setup. A Pb foil (1 × 3 cm^2, 1 × 2 cm^2 immersed) served as the cathode, while a Zn foil (or another active metal, 1 × 3 cm^2, 1 × 2 cm^2 immersed) served as the anode. The cell contained 10 mL of DMF with 0.10 M TBAP as the supporting electrolyte. In experiments where a Li anode was used, a piece of Li foil was first polished inside a glove box and immersed in the DMF electrolyte before being transferred

out of the glove box for assembly into the electrochemical cell. During electrolysis, the solution was stirred at 500 rpm with a magnetic stir bar, and CO_2 was continuously bubbled into the electrolyte at a flow rate of 20 sccm. Unless otherwise stated, the standard reaction conditions were a cell voltage of 3.0 V, an oxime concentration of 0.10 M, and a reaction time of 1 h.

Three-electrode measurements in the same undivided cell were carried out with a Ag wire serving as a quasi-reference electrode. Before each experiment, the resistance between the working and reference electrodes was measured by potentiostatic electrochemical impedance spectroscopy at open-circuit potential over a frequency range of 200 kHz to 1 Hz with a 10 mV perturbation amplitude. The solution resistance was obtained from the high-frequency intercept of the Nyquist plot on the real axis, and 100% iR compensation was subsequently applied during the measurement. All the other conditions were the same as the two-electrode measurements. The potential of the Ag wire quasi-reference electrode was calibrated against the Fc/Fc^+ redox couple by adding 5 mM Fc into the electrolyte after the electrochemical measurement and recording the cyclic voltammogram. Three-electrode measurements were also carried out in an H-cell using a Pb foil (1×3 cm^2, with 1×2 cm^2 immersed) as the working electrode, a Pt foil (1.5×1.5 cm^2, fully immersed) as the counter electrode, and a Ag wire quasi-reference electrode placed close to the working electrode in the cathode chamber. The catholyte was a DMF solution containing 0.10 M TBAP and 0.10 M BzOx, while the anolyte was DMF with 0.10 M TBAI. The two chambers were separated by a fine frit. CO_2 was continuously bubbled into the cathode chamber at a flow rate of 20 sccm with stirring at 500 rpm during measurement. Prior to each measurement, 100% iR compensation was applied.

The formulas used to calculate the conversion and FE values for the electroreductive carboxylation step and the overall two-step process are below, where $n_{final}(PhGly)$ is the amount of PhGly obtained after reaction, $n_{intermediate}(BzOx)$ is the amount of BzOx formed in the first step, $n_{initial}(PhCHO)$ is the amount of PhCHO before reaction, $Q_{electrocarboxylation}$ and $Q_{nitrite\ electroreduction}$ are the charges passed during the electrocarboxylation and nitrite electroreduction steps, respectively, and $n_{electrocarboxylation}(e)$ and $n_{nitrite\ electroreduction}(e)$ are the numbers of electrons transferred per molecule in the electrocarboxylation and nitrite electroreduction steps, respectively:

$$\mathrm{Conv.(electrocarboxylation)} = \frac{n_{final}(PhGly)}{n_{intermediate}(BzOx)} \times 100\%$$

$$\mathrm{Conv.(two-step)} = \frac{n_{final}(PhGly)}{n_{initial}(PhCHO)} \times 100\%$$

$$\mathrm{FE(electrocarboxylation)} = \frac{n_{final}(PhGly) \times n_{electrocarboxylation}(e) \times 96485\ C/mol}{Q_{electrocarboxylation}} \times 100\%$$

$$\mathrm{FE(two-step)} = \frac{n_{final}(PhGly) \times \left(n_{electrocarboxylation}(e) + n_{nitrite\ electroreduction}(e)\right) \times 96485\ C/mol}{Q_{electrocarboxylation} + Q_{nitrite\ electroreduction}} \times 100\%$$

$$n_{electrocarboxylation}(e) = 4, \qquad n_{nitrite\ electroreduction}(e) = 4$$

Synthesis of 2-hydroxyamino-2-phenylacetic acid

2-Bromo-2-phenylacetic acid and NH_2OH were mixed in deionized water to give final concentrations of 0.10 M and 0.20 M, respectively. The mixture was stirred at 40 °C for 1 h, then cooled to room temperature, and the product was extracted with dichloromethane. The organic phase was then removed under reduced pressure at room temperature to afford 2-hydroxyamino-2-phenylacetic acid. The ^1H NMR spectrum of the product is shown in Fig. S21.

Electroreductive carboxylation of benzaldimine

Benzaldimine was generated in situ in the electrolyte prior to electrolysis. NH_3 gas was continuously bubbled for 1 h into a 10 mL DMF electrolyte containing 0.10 M PhCHO and 0.10 M TBAP, forming benzaldimine (Fig. S24). The resulting solution was directly used as the electrolyte for electrolysis in an undivided cell. A Pb foil (1 × 3 cm^2, with 1 × 2 cm^2 immersed) served as the cathode, and a Zn foil (1 × 3 cm^2, with 1 × 2 cm^2 immersed) served as the anode. Electrolysis was performed at a cell potential of 3.0 V for 1 h under continuous CO_2 bubbling (20 sccm) and stirring at 500 rpm.

Analysis of electroreductive carboxylation products

To analyze products in the electrolyte, the electrolyte suspension after electrolysis was well mixed and 50 μL was taken out to mix with 50 μL of 1.0 M HCl, resulting in a clear solution. Deionized water was then added to bring the total volume to 450 μL, followed by the addition of 50 μL of D_2O containing 0.01 M MeCN as an internal standard. The resulting 500 μL solution was used for NMR analysis. To analyze products in the precipitate, the electrolyte after electrolysis was first filtered to collect the solid. The obtained solid was washed thoroughly with DMF and then acetone to remove TBAP and other organic residues. After drying, a portion of the solid was collected for X-ray diffraction analysis. The remaining solid was then dissolved in 2 mL of 1.0 M HCl and filtered to remove insoluble residues. A 450 μL aliquot of the clear filtrate was mixed with 50 μL of D_2O containing 0.01 M MeCN as an internal standard to prepare an NMR sample. 50 μL of the electrolyte filtrate was mixed with 50 μL of 1.0 M HCl and 400 μL of deionized water to prepare an analyte solution. Then, 450 μL of this solution was combined with 50 μL of D_2O containing 0.01 M MeCN to obtain an NMR sample for analysis of the used electrolyte.

Supplementary Figures

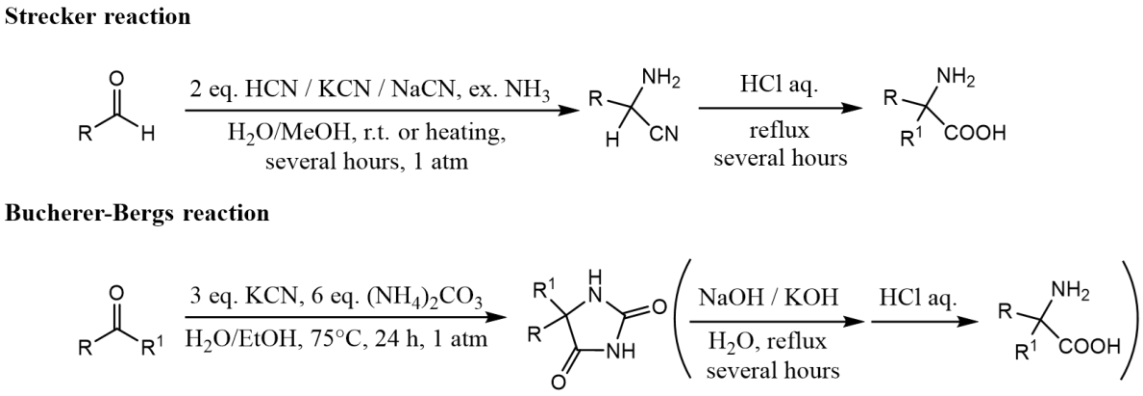

Supplementary Figure 1. Representative conditions of Strecker and Bucherer–Bergs reactions.

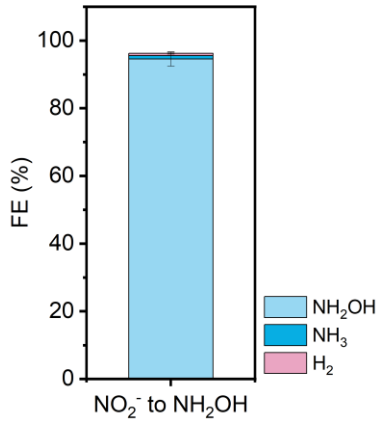

Supplementary Figure 2. Product distribution for NO_2^- electroreduction over Pd cathode at −0.1 V vs RHE in 0.1 M phosphate buffer solution (pH 7) containing 0.1 M KNO_2. Product quantification was carried out following our previous work (ACS Catal. 2022, 12, 9135). Data are presented as mean ± s.d. (n = 3 independent experiments).

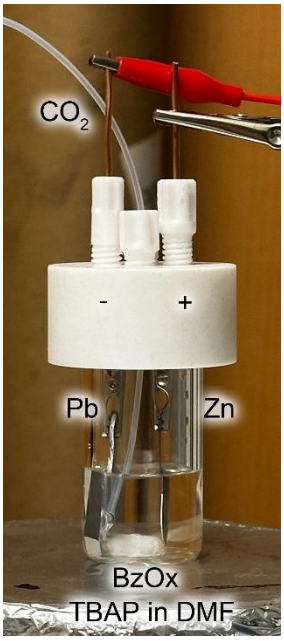

Supplementary Figure 3. Photograph of two-electrode undivided cell used for electroreductive carboxylation.

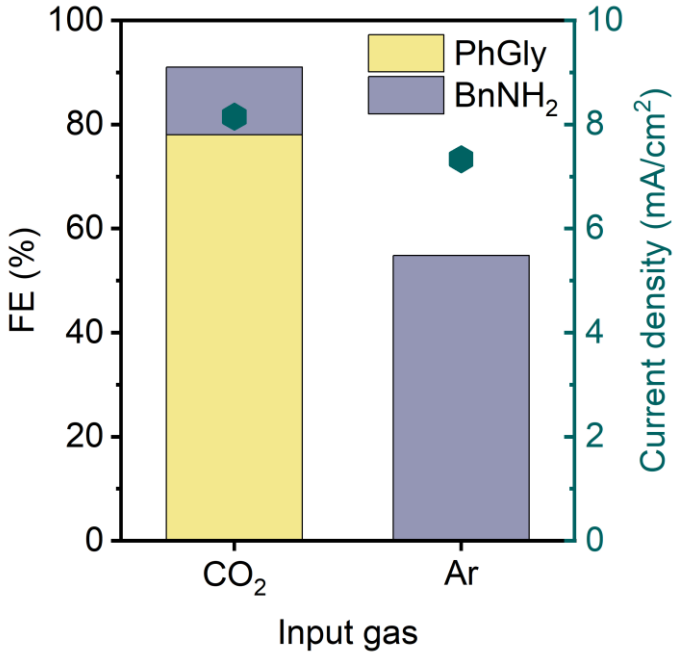

Supplementary Figure 4. FEs and total current densities for electroreductive carboxylation of BzOx in CO_2 vs Ar gas atmosphere.

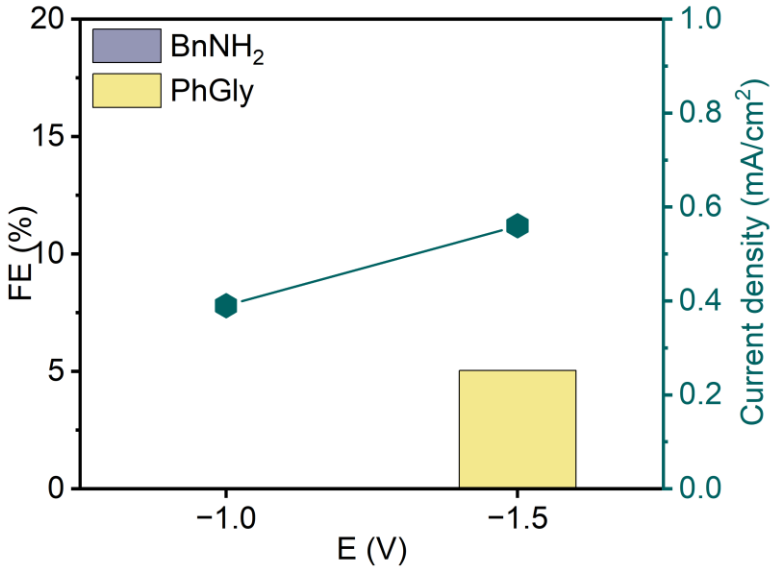

Supplementary Figure 5. FEs and total current densities for electrochemical reductive carboxylation conducted at −1.0 and −1.5 V.

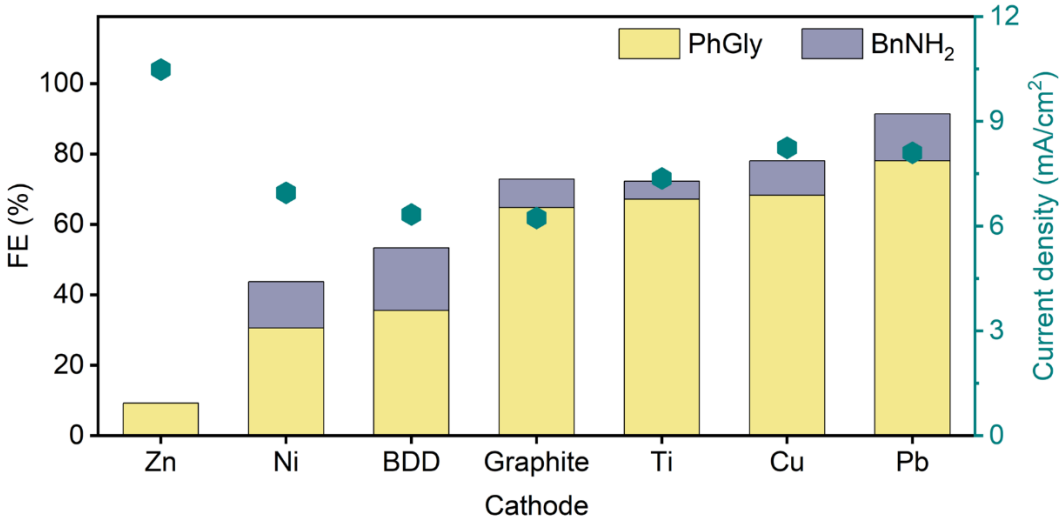

Supplementary Figure 6. FEs and total current densities for electroreductive carboxylation of BzOx using different cathodes (all at −3.0 V).

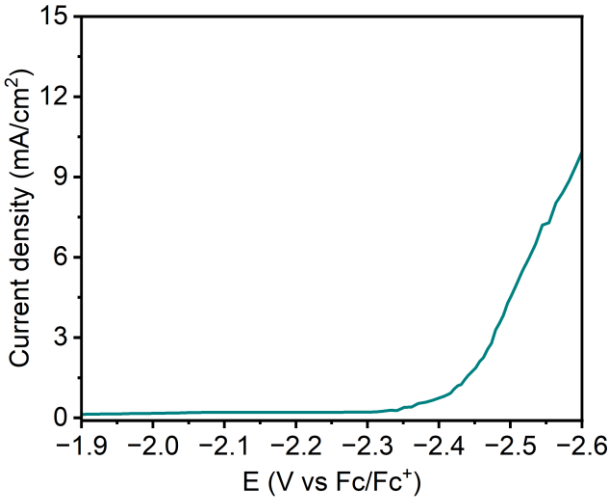

Supplementary Figure 7. Linear sweep voltammogram at a scan rate of 10 mV/s for electroreductive carboxylation of BzOx in a three-electrode undivided cell.

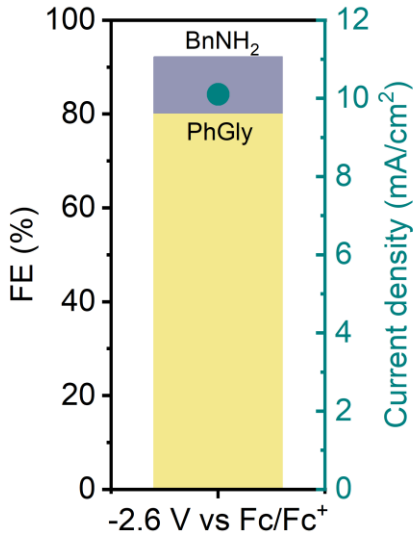

Supplementary Figure 8. FEs and total current density for electroreductive carboxylation of BzOx at −2.6 V vs Fc/Fc$^+$ measured in a three-electrode undivided cell.

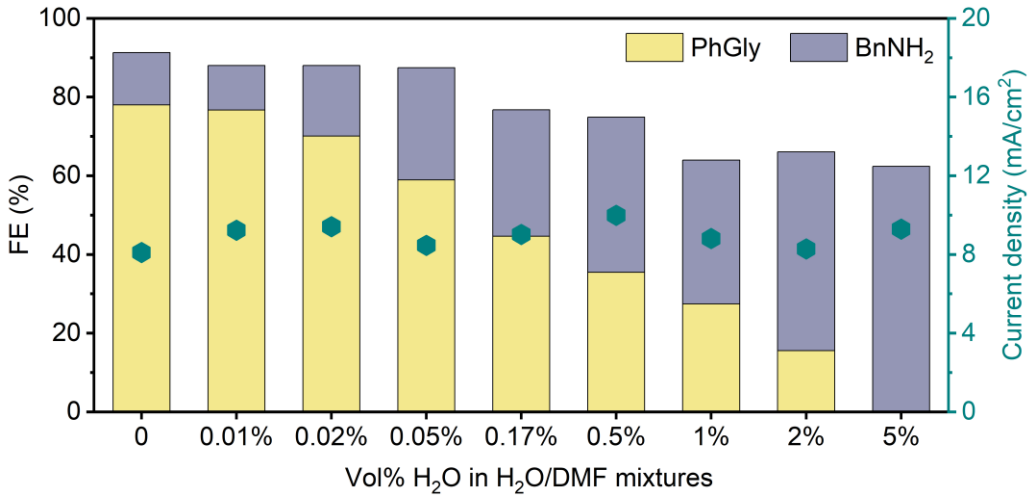

Supplementary Figure 9. FEs and total current densities for electroreductive carboxylation of BzOx in H_2O/DMF mixed electrolyte with varied volume percentages of H_2O.

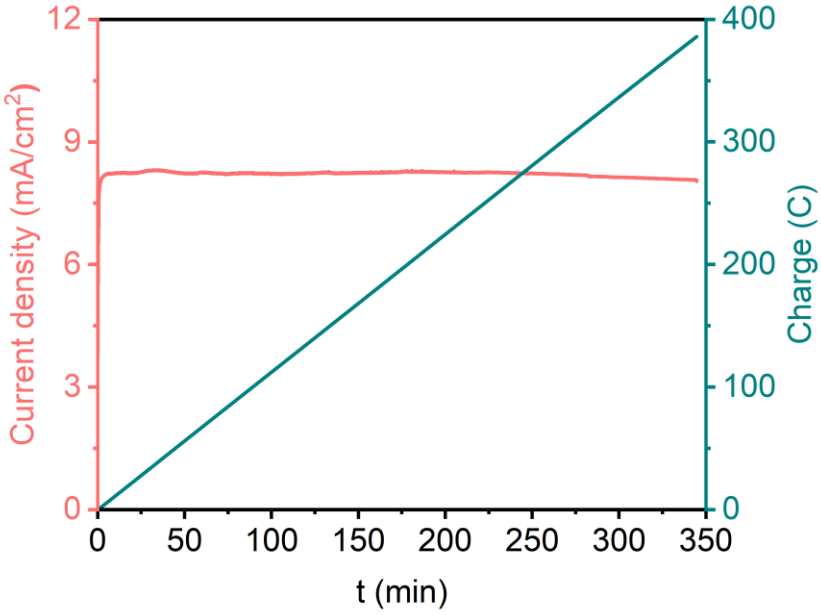

Supplementary Figure 10. Total current density and accumulated charge during electroreductive carboxylation until the theoretical charge corresponding to 100% conversion is reached.

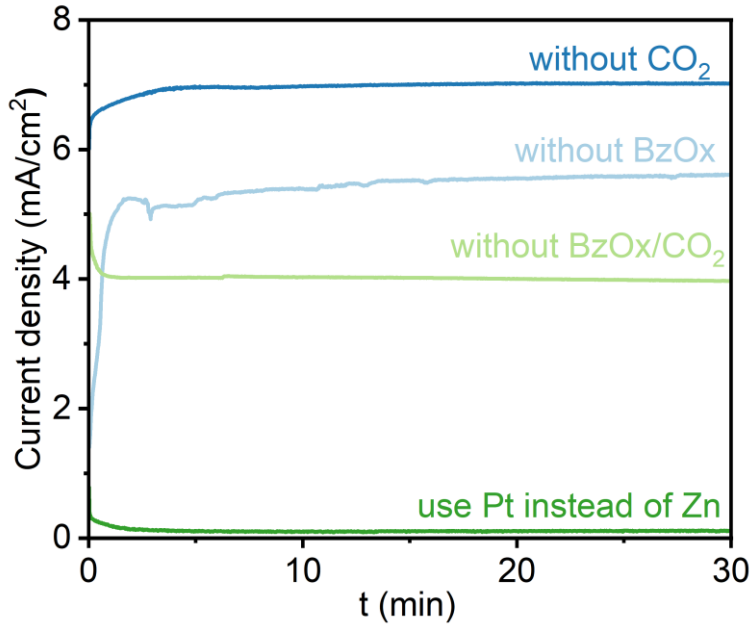

Supplementary Figure 11. Total current density during 30 min electrolysis under various control conditions, including absence of BzOx, absence of CO_2, absence of both BzOx and CO_2, and replacement of the Zn anode with Pt, while keeping all other conditions identical.

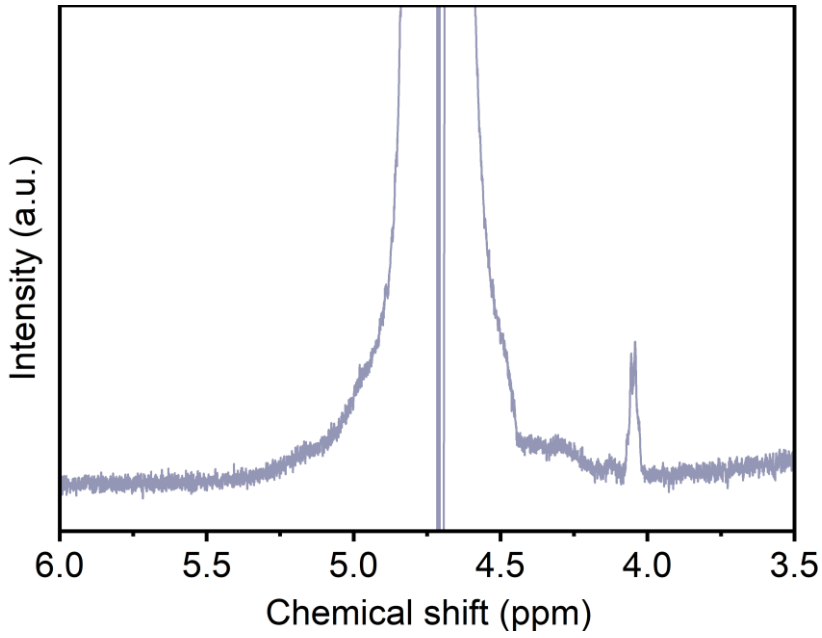

Supplementary Figure 12. ^{1}H NMR spectrum of electrolyte after electrolysis under standard electroreductive carboxylation conditions but in the absence of CO_2.

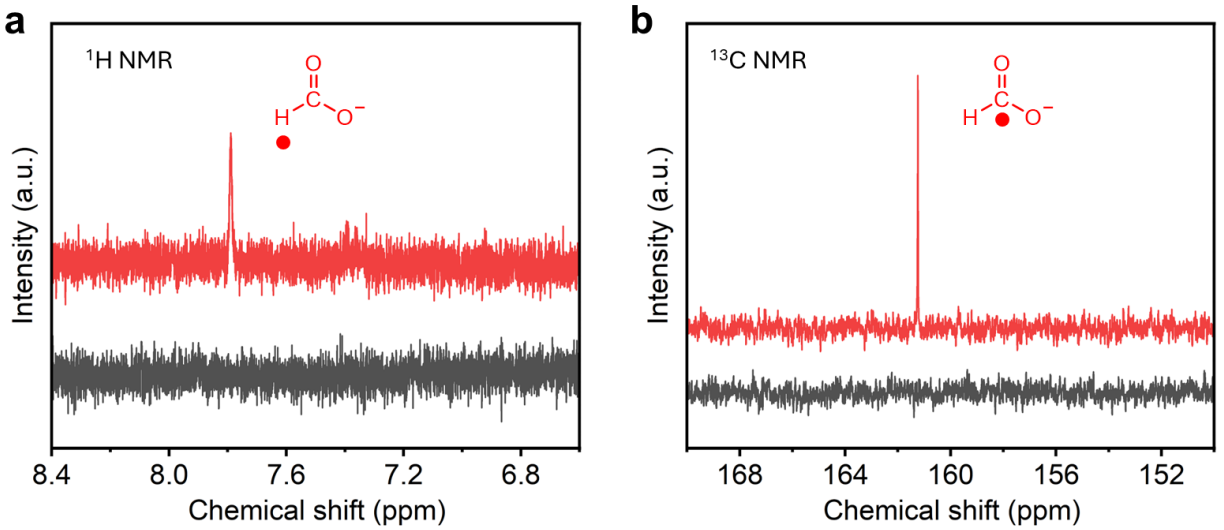

Supplementary Figure 13. (a) ^{1}H and (b) ^{13}C NMR spectra of precipitates after electrolysis under standard electroreductive carboxylation conditions in the absence of BzOx, with (red trace) or without (gray trace) CO_2.

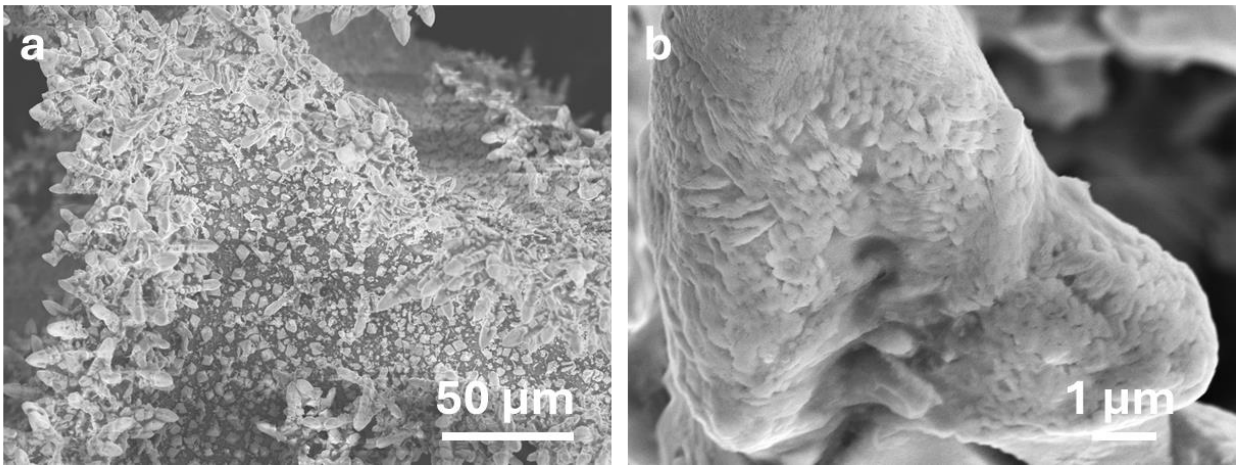

Supplementary Figure 14. SEM images of Pb/Ni foam at (a) low and (b) high magnifications.

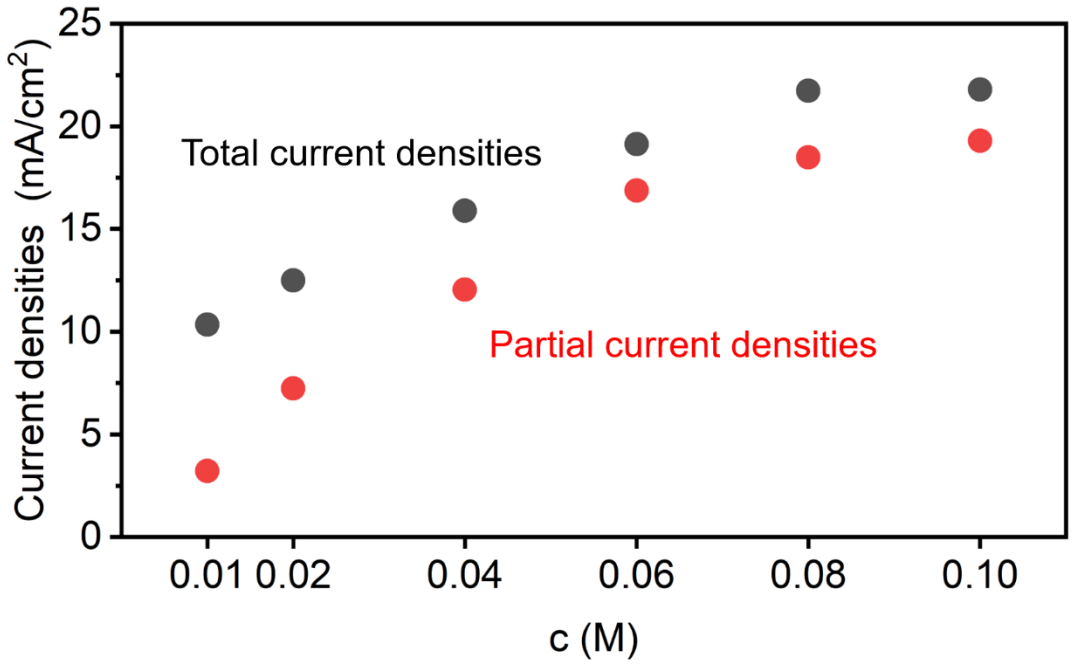

Supplementary Figure 15. Total current densities and PhGly partial current densities for 20 min reductive carboxylation electrolysis with a Pb/Ni foam working electrode at varied BzOx concentrations.

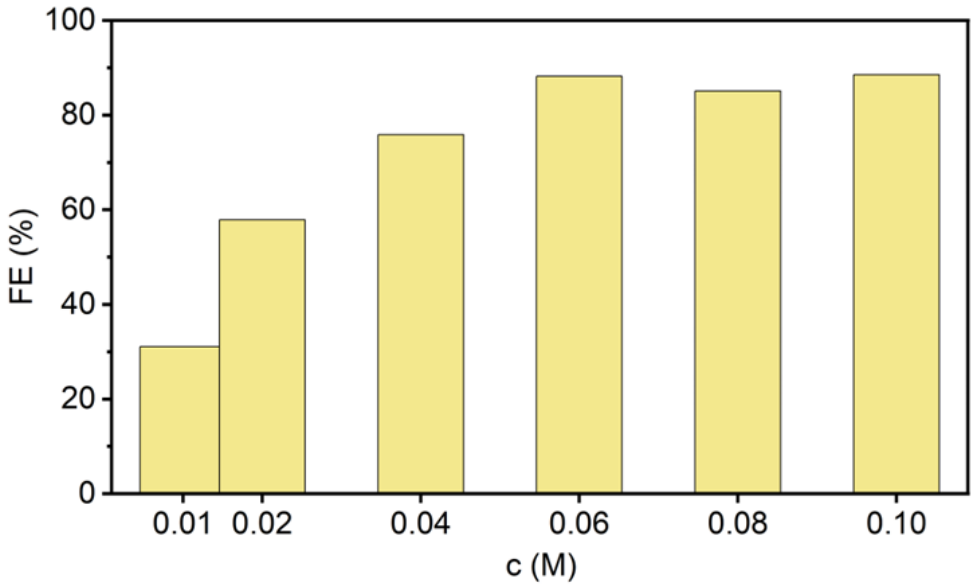

Supplementary Figure 16. PhGly FEs for 20 min reductive carboxylation electrolysis with a Pb/Ni foam working electrode at varied BzOx concentrations.

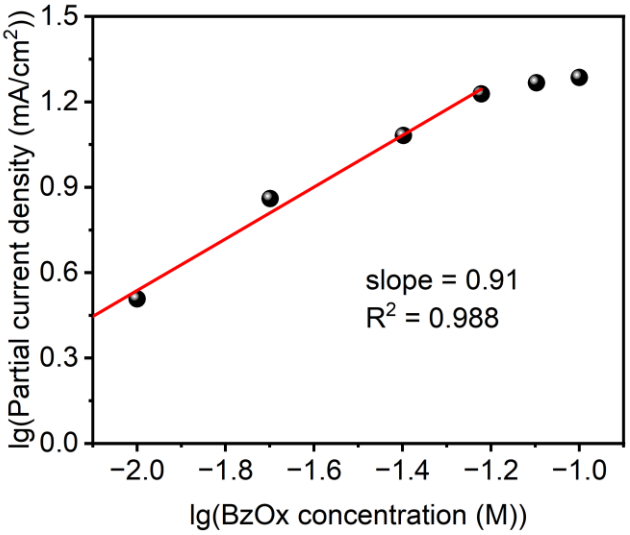

Supplementary Figure 17. Logarithmic plot of PhGly partial current density vs BzOx concentration obtained from 20 min reductive carboxylation electrolysis with a Pb/Ni foam working electrode.

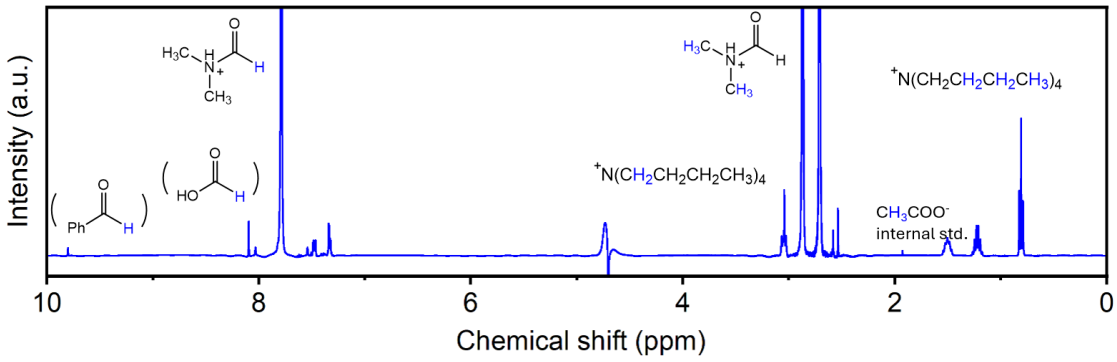

Supplementary Figure 18. ^{1}H NMR spectrum of electrolyte after electrolysis and filtration. The signals of PhCHO and HCOOH are from BzOx hydrolysis and CO_2 reduction, respectively.

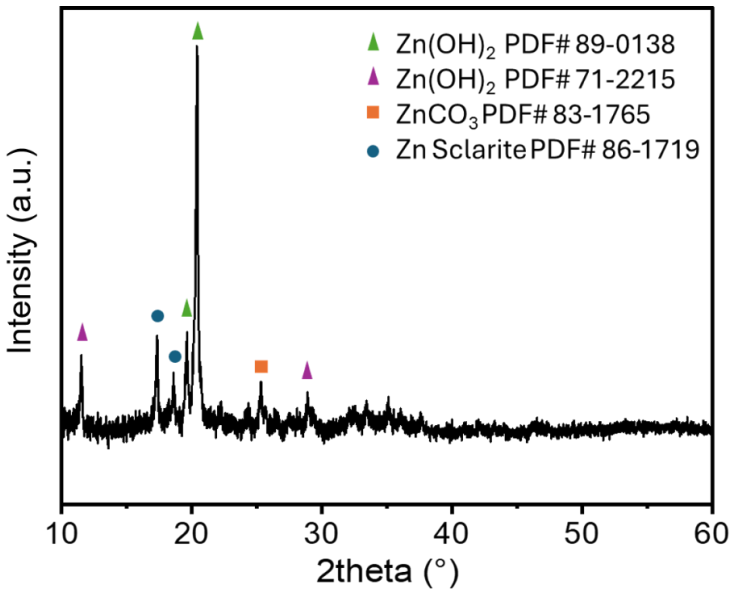

Supplementary Figure 19. X-ray diffraction pattern of precipitate from electroreductive carboxylation of BzOx.

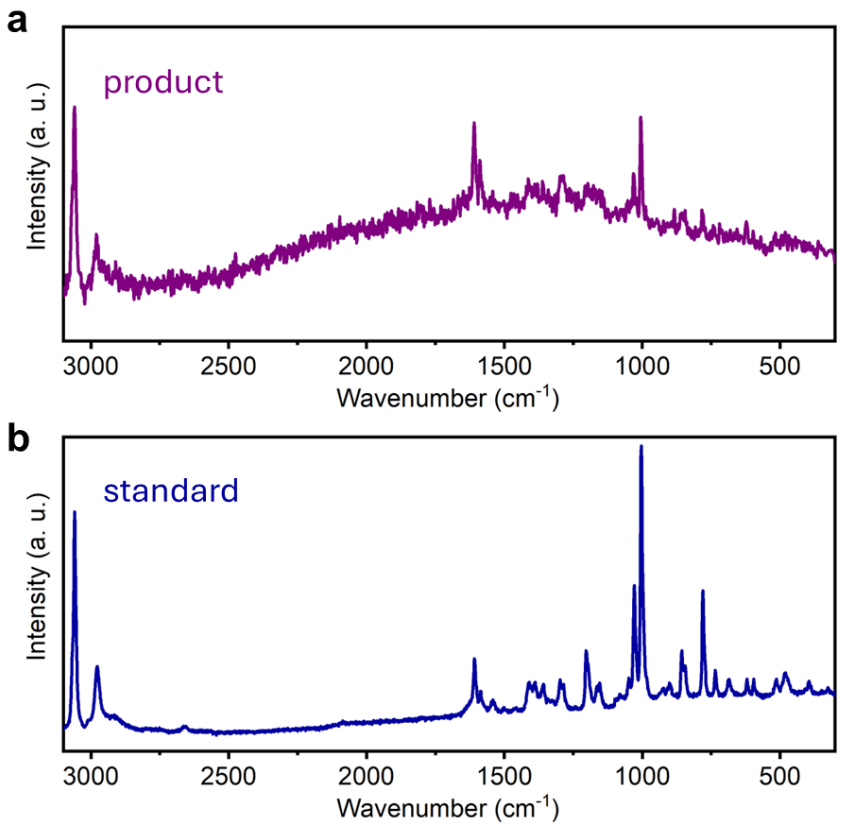

Supplementary Figure 20. Raman spectra of (a) the final PhGly product and (b) a standard PhGly sample (purchased from Sigma-Aldrich).

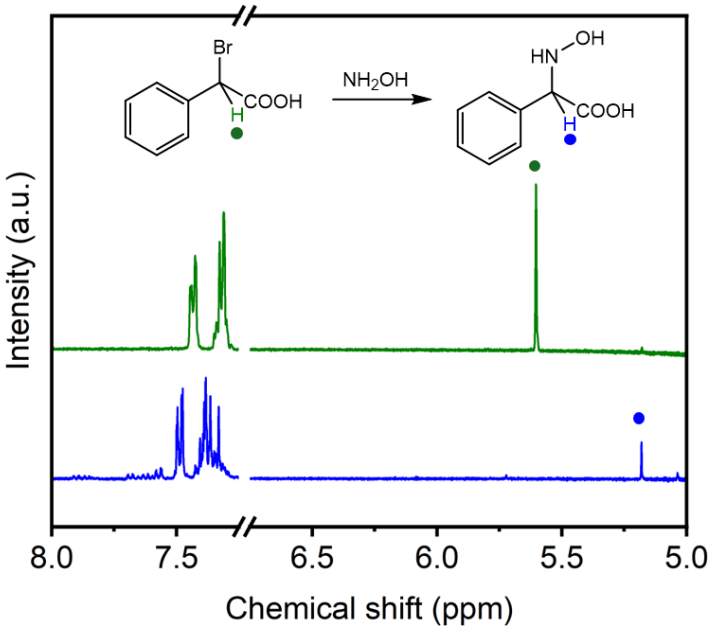

Supplementary Figure 21. ^{1}H NMR spectra showing 2-bromo-2-phenylacetic acid and its conversion to 2-hydroxyamino-2-phenylacetic acid in aqueous solution.

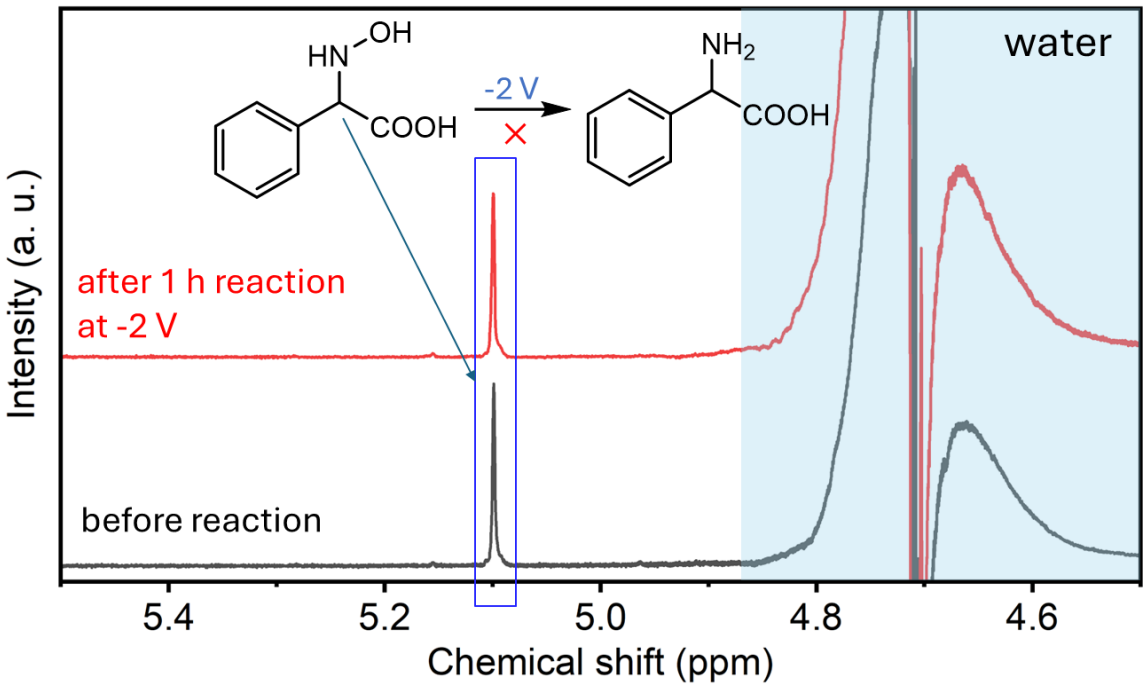

Supplementary Figure 22. ^{1}H NMR spectra of electrolyte before and after electroreduction of 2-hydroxyamino-2-phenylacetic acid conducted at −2.0 V for 1 h using a Pb foil cathode and a Zn foil anode in DMF containing 0.10 M TBAP.

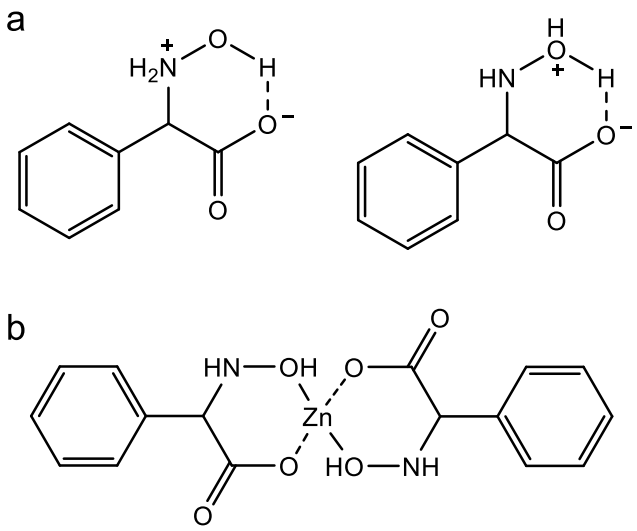

Supplementary Figure 23. Schematic illustration of 2-hydroxyamino-2-phenylacetic acid forming stable six-membered ring structures via (a) intramolecular hydrogen bonding or (b) coordination to a zinc ion.

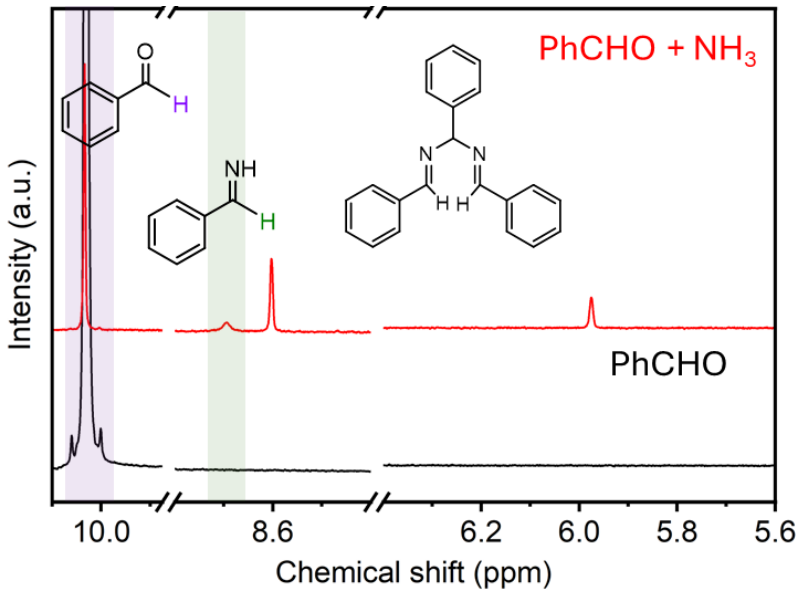

Supplementary Figure 24. ^{1}H NMR spectra showing PhCHO and its conversion to BzIm via reaction with NH_3.

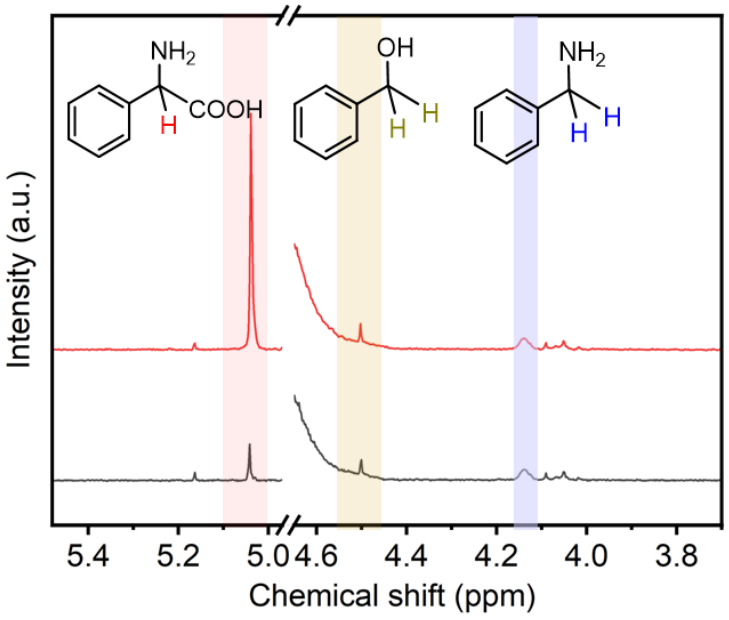

Supplementary Figure 25. ^{1}H NMR spectra of electrolyte after electroreductive carboxylation of BzIm. Black: original; red: with PhGly added.

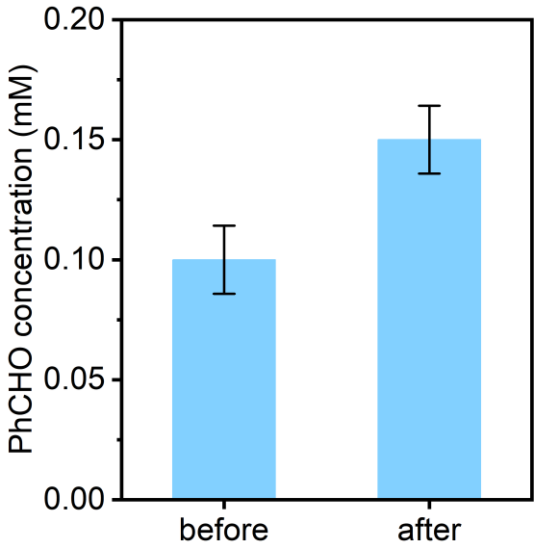

Supplementary Figure 26. Measured PhCHO concentrations in the electrolyte before and after electroreductive carboxylation of BzOx. The electrolyte was treated with 0.1 M aqueous NaOH before PhCHO quantification, which was sufficient to dissolve the precipitate but not strong enough to hydrolyze unreacted BzOx. Data are presented as mean ± s.d. (n = 2 independent experiments).

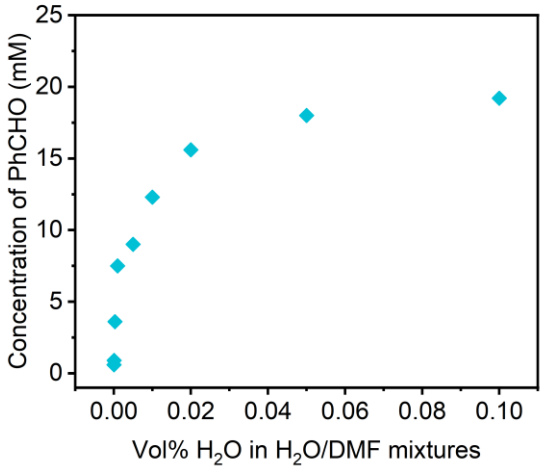

Supplementary Figure 27. Measured PhCHO concentrations in the electrolyte after electroreductive carboxylation of BzOx in H_2O/DMF mixed electrolyte with varied volume percentages of H_2O. The electrolyte was treated with 0.1 M aqueous NaOH before PhCHO quantification.

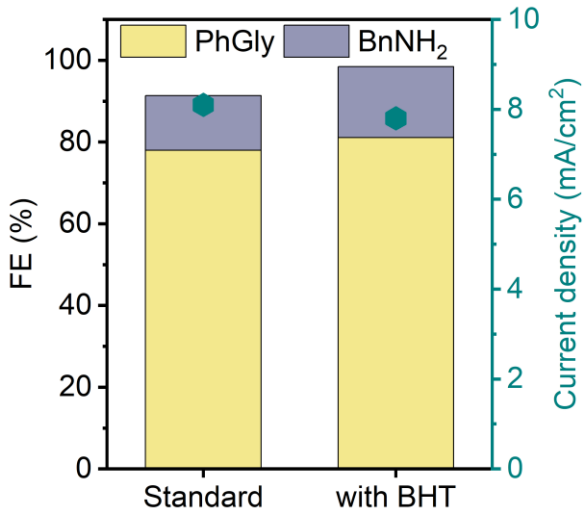

Supplementary Figure 28. FEs and total current densities for electroreductive carboxylation of BzOx without (left) vs with (right) 0.1 M BHT added to the electrolyte.

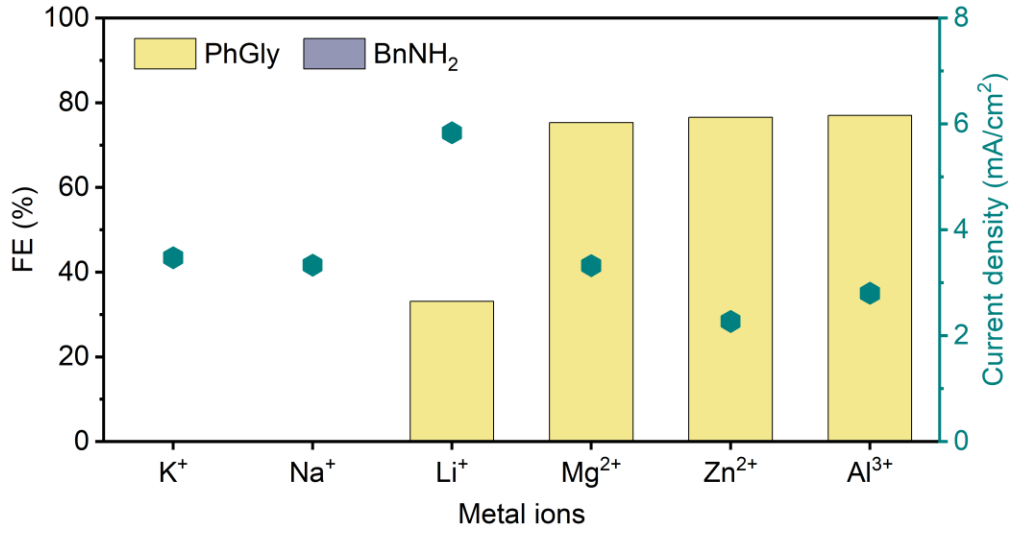

Supplementary Figure 29. FEs and total current densities for electroreductive carboxylation of BzOx performed at −3.1 V vs Fc/Fc^+ for 1 h in a three-electrode H-cell with 50 mM of anhydrous $KClO_4$, $NaClO_4$, $LiClO_4$, $MgCl_2$, $Zn(OTf)_2$, or $AlCl_3$ added in the catholyte.

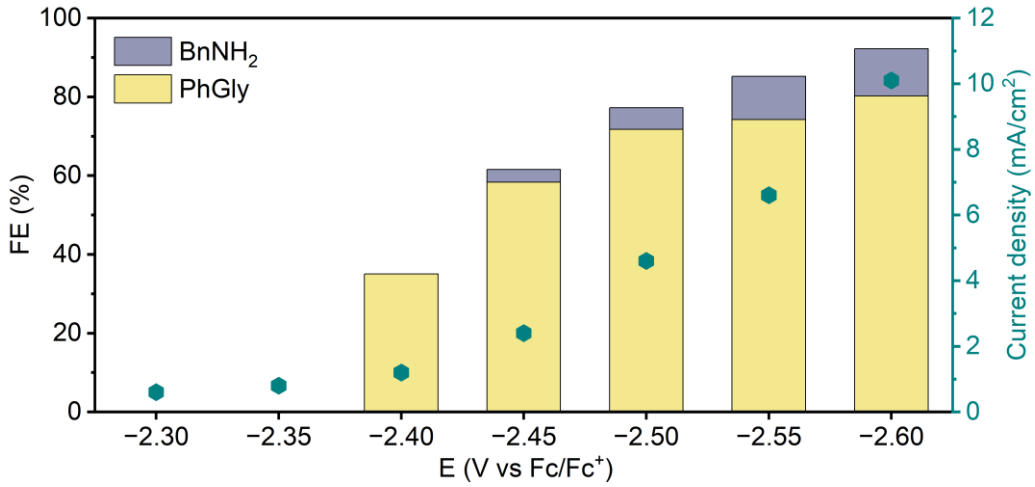

Supplementary Figure 30. FEs and total current densities for electroreductive carboxylation of BzOx at varied electrode potentials measured in a three-electrode undivided cell.

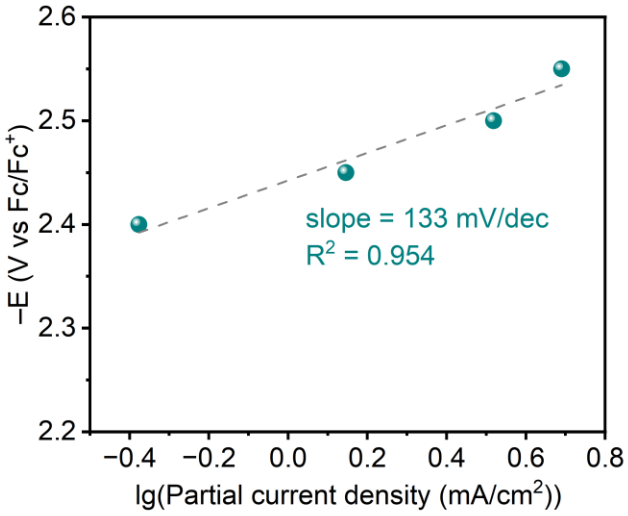

Supplementary Figure 31. Tafel analysis for electroreductive carboxylation of BzOx.

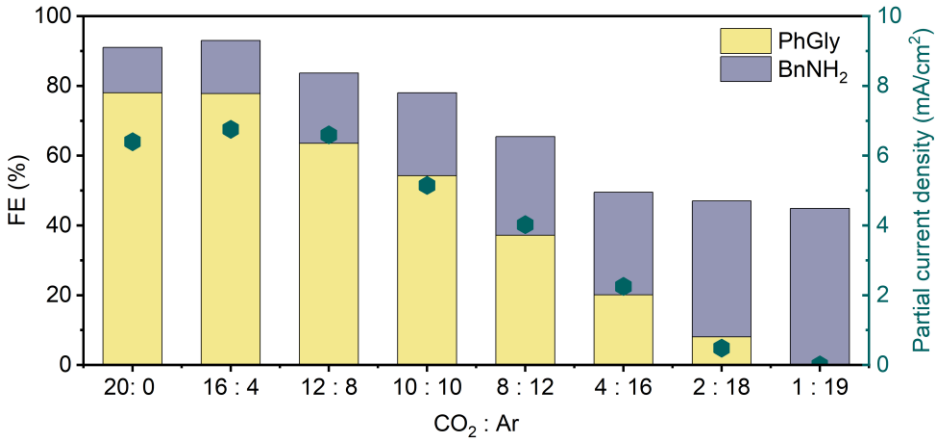

Supplementary Figure 32. FEs and PhGly partial current densities for electroreductive carboxylation of BzOx in CO_2/Ar mixed atmosphere.

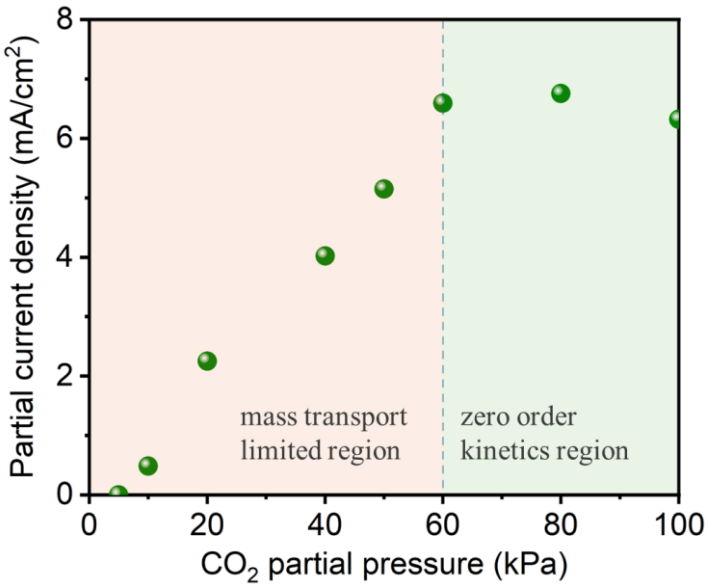

Supplementary Figure 33. Dependence of PhGly partial current density on CO_2 partial pressure for electroreductive carboxylation of BzOx.

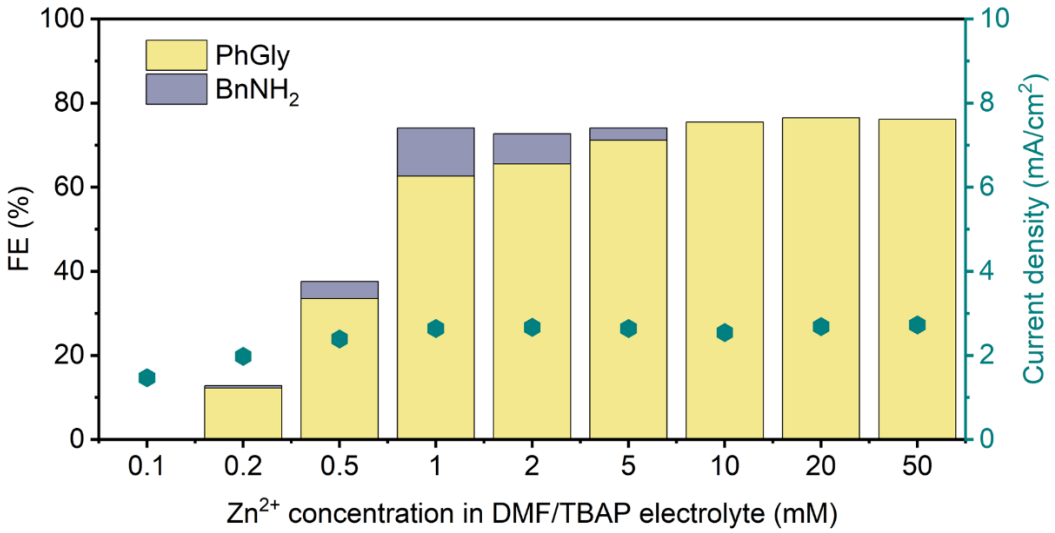

Supplementary Figure 34. FEs and total current densities for electroreductive carboxylation of BzOx performed at −3.1 V vs Fc/Fc^+ for 1 h in a three-electrode H-cell with varied amount of anhydrous $Zn(OTf)_2$ added in the catholyte.

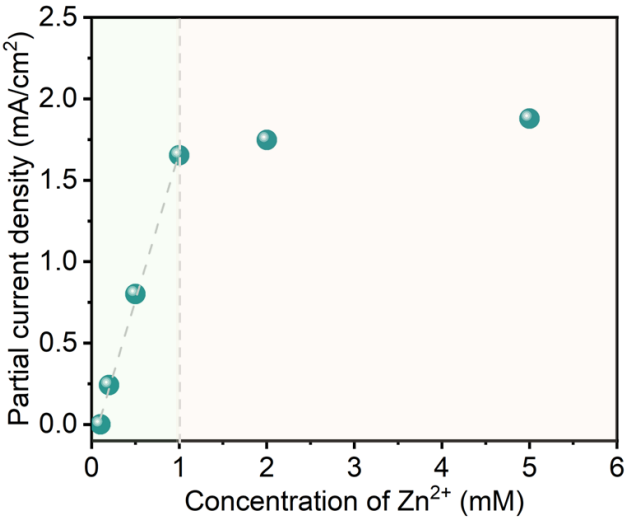

Supplementary Figure 35. Partial current density of PhGly vs Zn^{2+} concentration in catholyte for electroreductive carboxylation of BzOx at −3.1 V vs Fc/Fc^+ measured in a three-electrode H-cell.

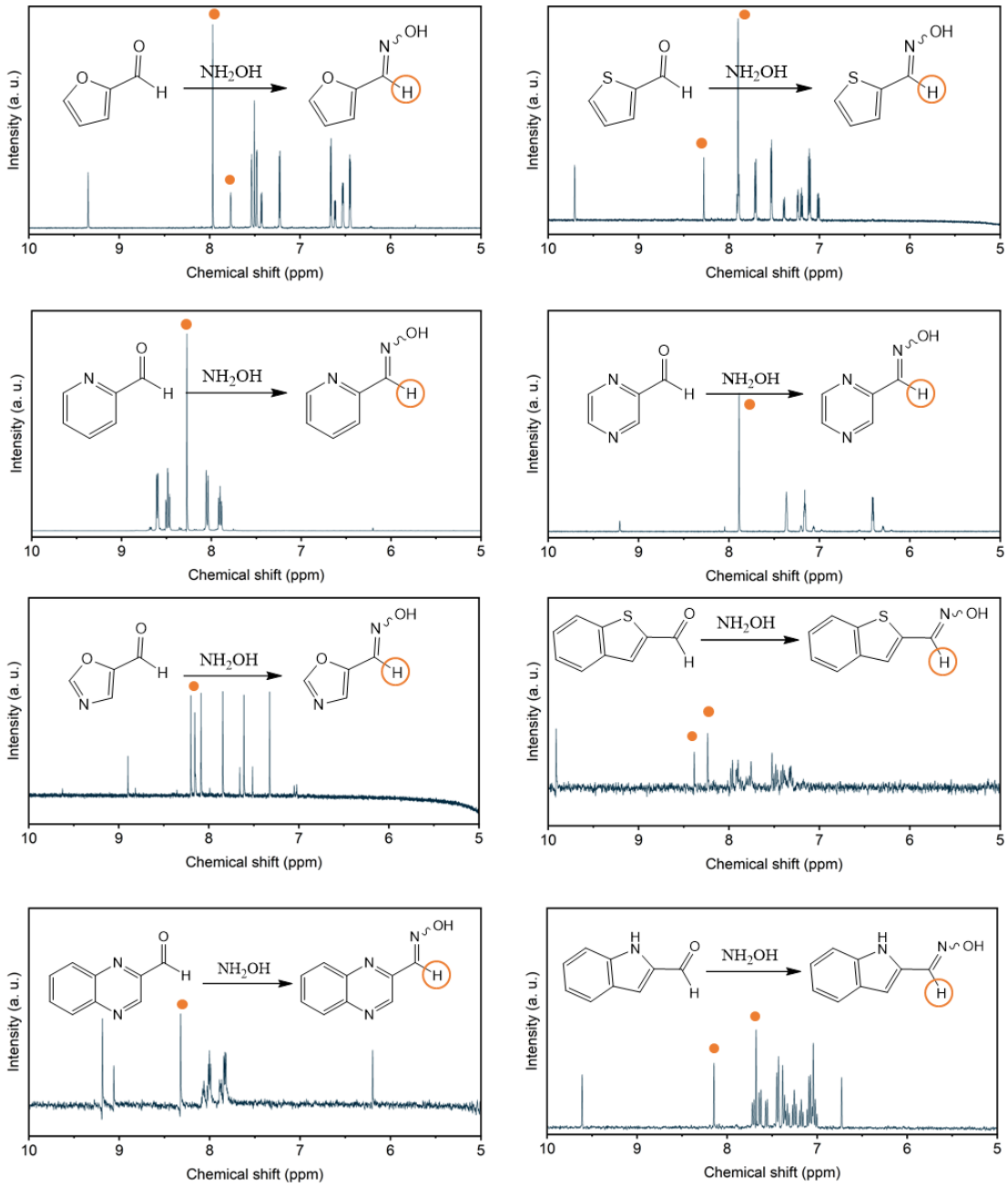

Supplementary Figure 36. ^{1}H NMR characterization of aryl oximes synthesized from aryl aldehydes and NH_2OH.

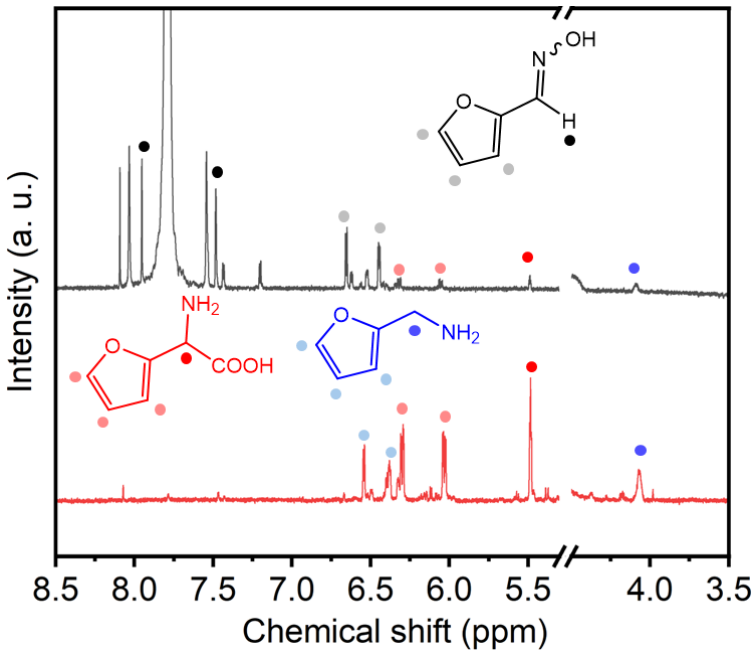

Supplementary Figure 37. [1]H NMR spectra of products from electroreductive carboxylation of furan-2-aldoxime. Black: post-electrolysis electrolyte; red: filtered solid product re-dissolved in HCl.

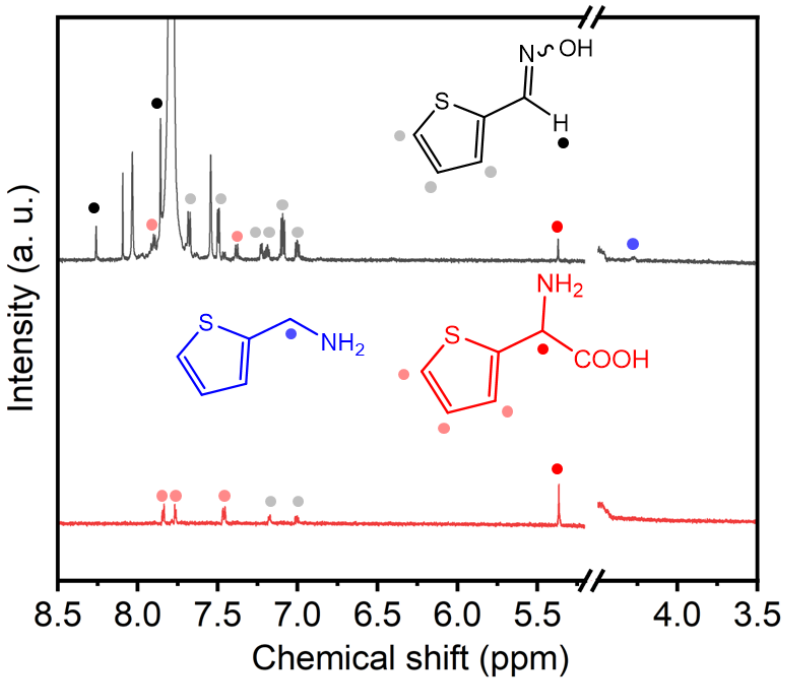

Supplementary Figure 38. [1]H NMR spectra of products from electroreductive carboxylation of thiophene-2-aldoxime. Black: post-electrolysis electrolyte; red: filtered solid product re-dissolved in HCl.

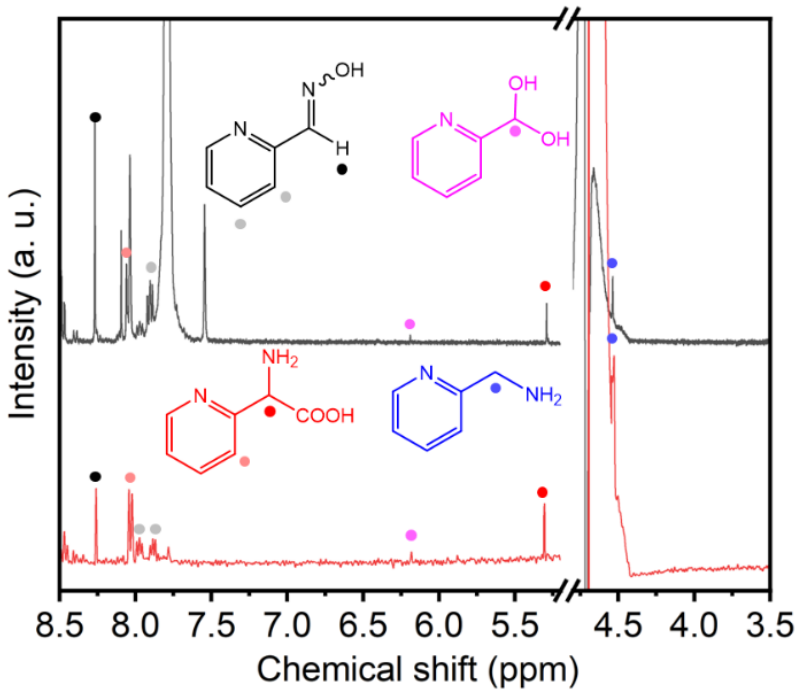

Supplementary Figure 39. ^{1}H NMR spectra of products from electroreductive carboxylation of pyridine-2-aldoxime. Black: post-electrolysis electrolyte; red: filtered solid product re-dissolved in HCl.

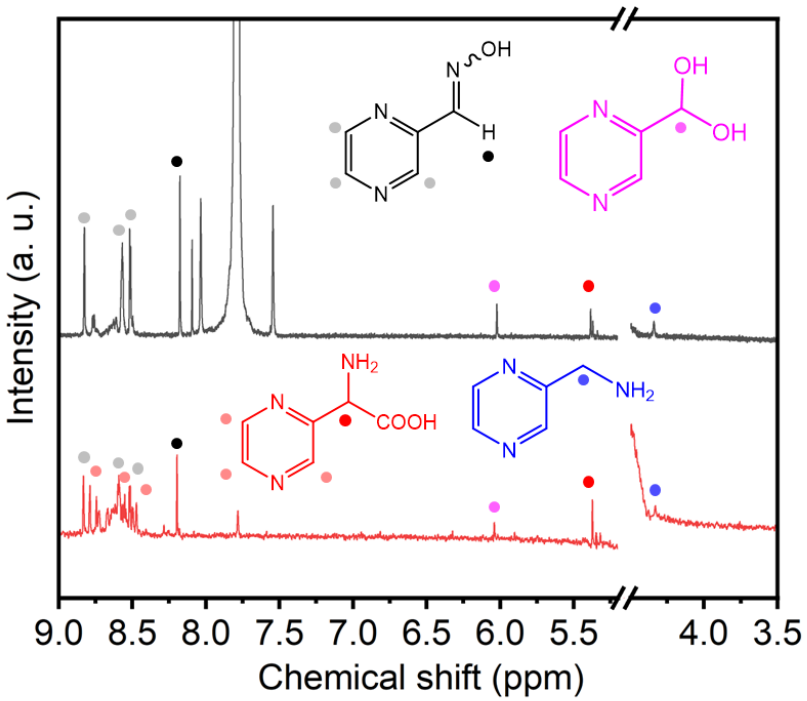

Supplementary Figure 40. ^{1}H NMR spectra of products from electroreductive carboxylation of pyrazine-2-aldoxime. Black: post-electrolysis electrolyte; red: filtered solid product re-dissolved in HCl.

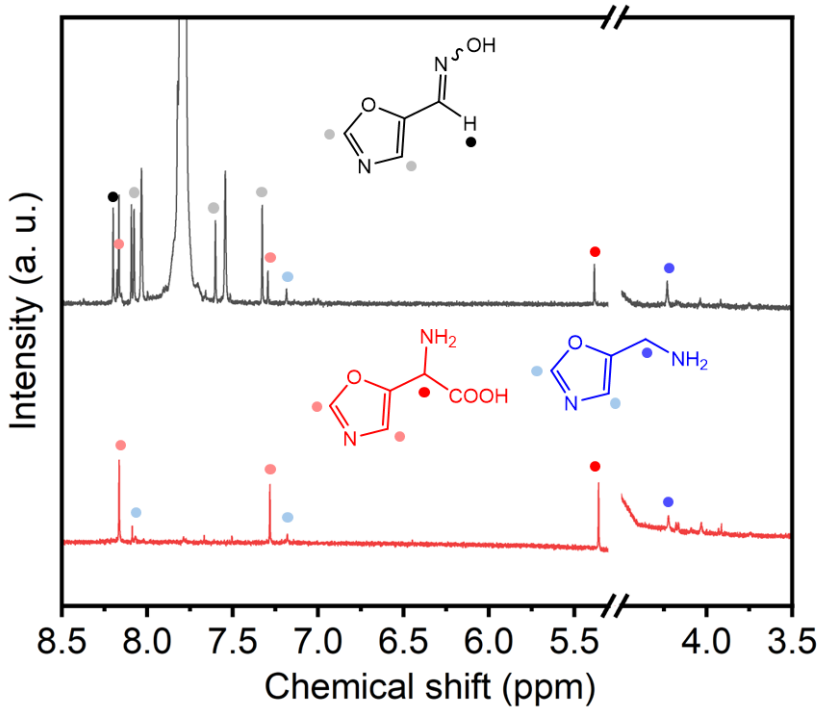

Supplementary Figure 41. ^{1}H NMR spectra of products from electroreductive carboxylation of oxazole-5-aldoxime. Black: post-electrolysis electrolyte; red: filtered solid product re-dissolved in HCl.

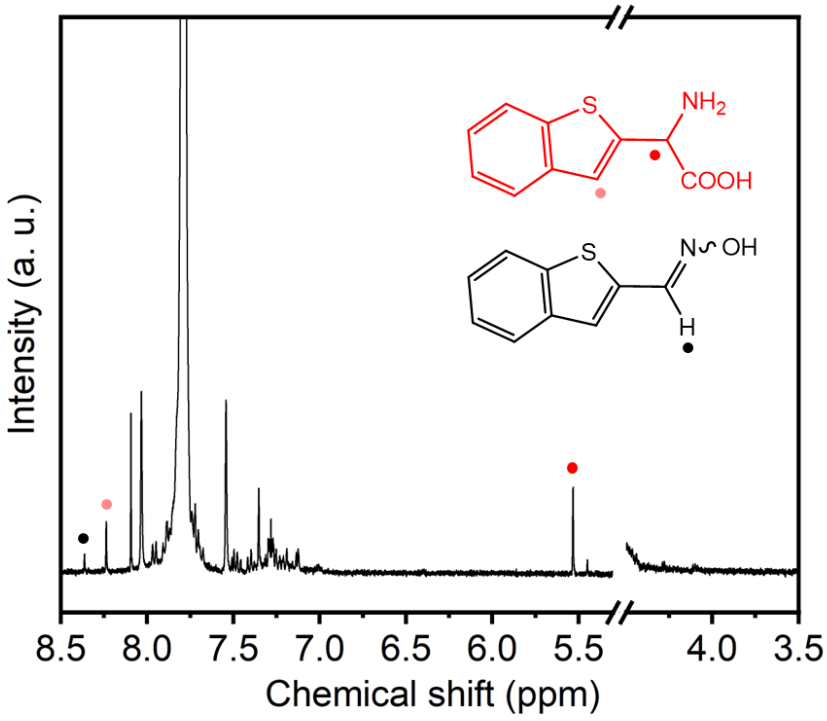

Supplementary Figure 42. ^{1}H NMR spectrum of electrolyte after electroreductive carboxylation of benzothiophene-2-aldoxime.

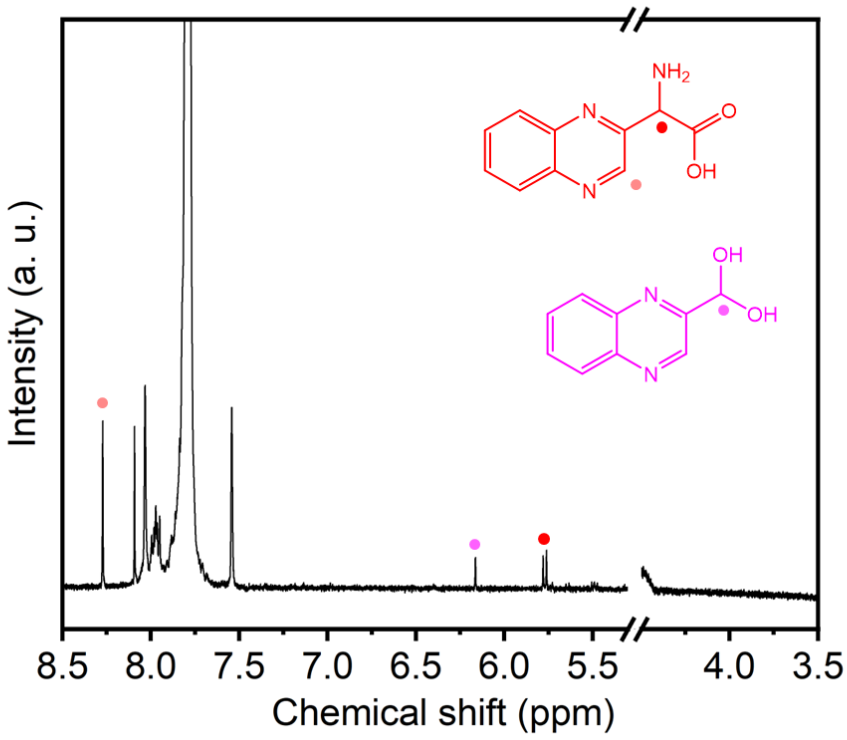

Supplementary Figure 43. ^{1}H NMR spectrum of electrolyte after electroreductive carboxylation of quinoxaline-2-aldoxime.

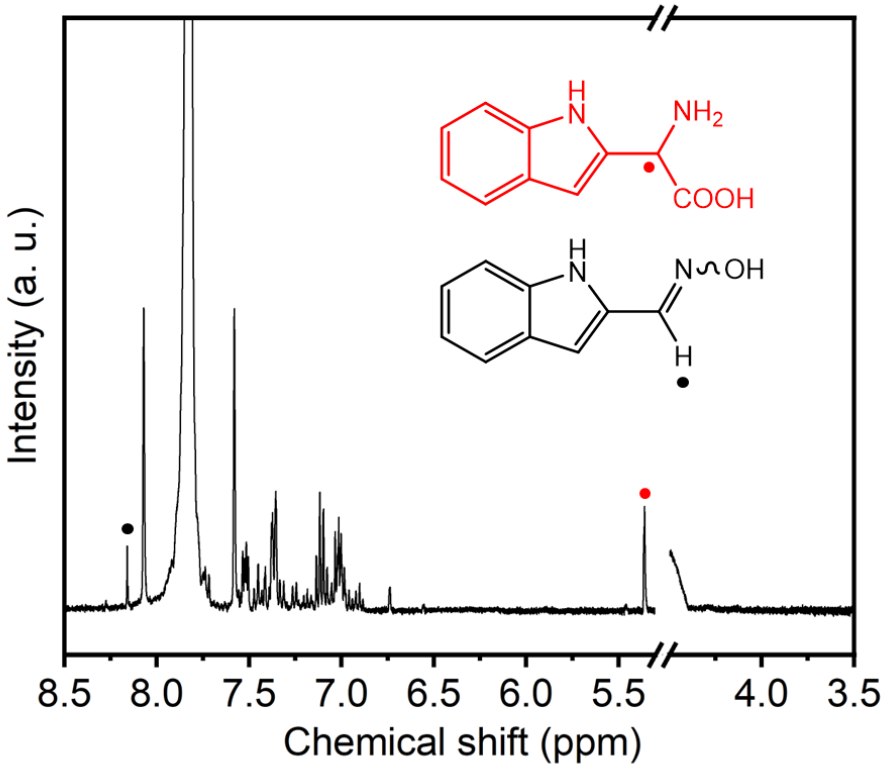

Supplementary Figure 44. ^{1}H NMR spectrum of electrolyte after electroreductive carboxylation of indole-2-aldoxime.

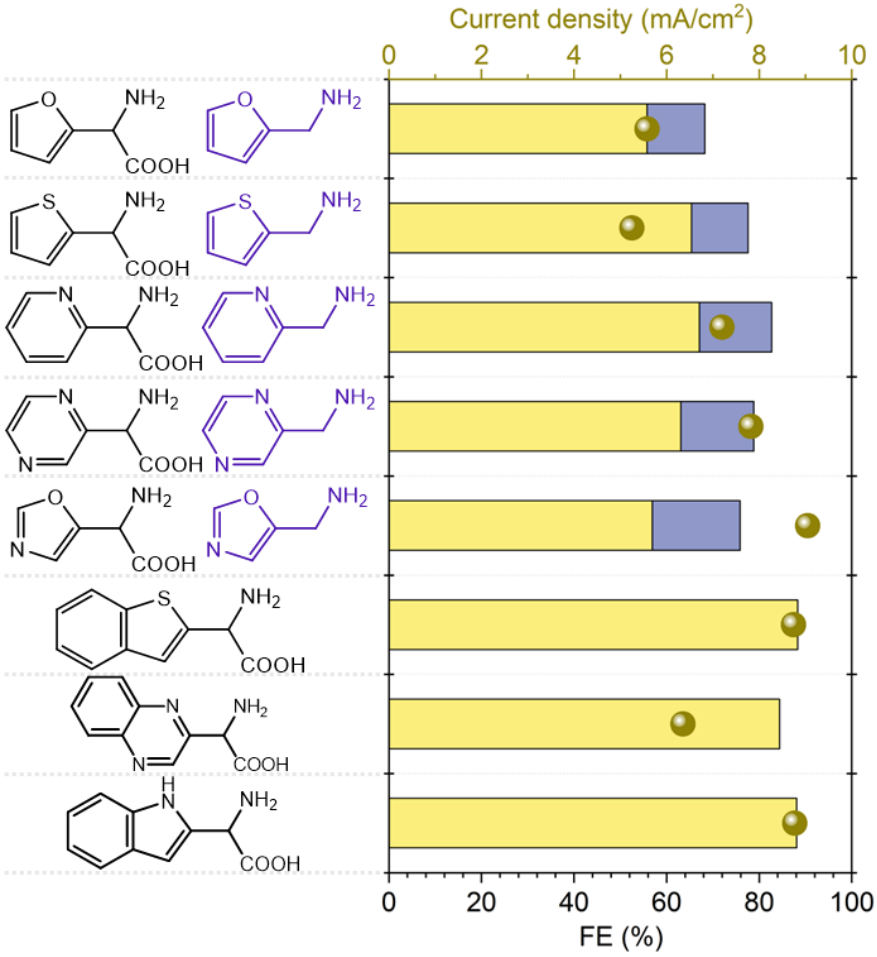

Supplementary Figure 45. FEs and total current densities for electroreductive carboxylation of various heteroaromatic aldoximes.

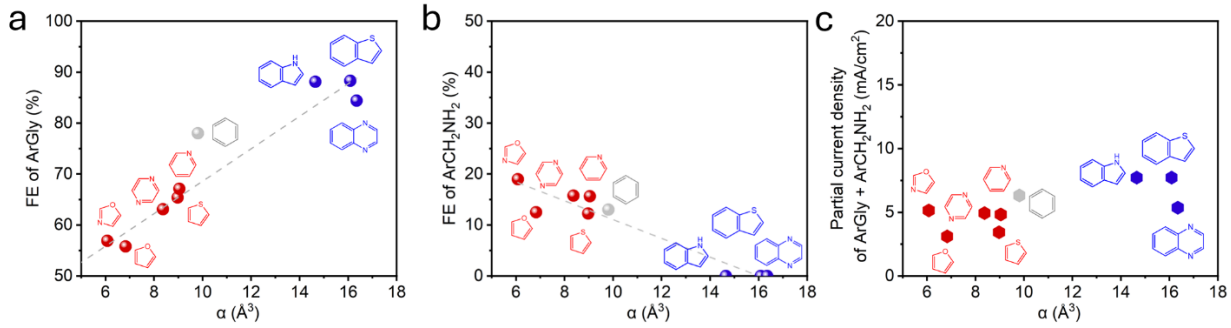

Supplementary Figure 46. Correlation of molecular polarizability (α) of Ar−H with (a) ArGly FE, (b) $ArCH_2NH_2$ FE, and (c) combined partial current density of ArGly and $ArCH_2NH_2$ in electroreductive carboxylation reactions of ArCH=NOH. The static isotropic polarizabilities were determined via density functional theory calculations at the B3LYP/6-311+G(d,p) level with the Polar keyword in Gaussian 16, utilizing fully optimized geometries.

Supplementary Tables

Supplementary Table 1. Comparison with amino acid electrosynthesis based on α-keto acid substrates.

Category	**Methods based on α-keto acids/oxalic acids**	**This work**
Organic substrate	Pre-functionalized substrates (α-keto acids, α-hydroxyl acids, and oxalic/glyoxylic acid)	Simple aromatic aldehydes
Substrate origin	Typically derived from biomass upgrading or chemical pre-synthesis	Widely available commodity or biomass chemicals
Substrate cost	Higher, due to functionalization and limited availability	Lower, due to broad availability of aldehydes
Nitrogen source	NO_3^-/NO_2^-/NO	NO_2^-, extendable to NO_3^-/NO
Carbon source	Already in the organic substrate (no CO_2 incorporation)	CO_2 (directly incorporated)
Use of environmental waste feedstocks	NO_x^{y-} utilization	Dual utilization of CO_2 and NO_2^-
Overall feedstock sustainability	Limited by reliance on pre-functionalized organic acids	Higher sustainability due to simple inputs and waste valorization

Supplementary Table 2. Comparison with amino acid electrosynthesis based on carboxylation of imines.

Category	**Methods based on electrochemical carboxylation of imines**	**This work**
Product type	N-substituted (N-aryl or N-acyl) α-amino acids	Unsubstituted (free) arylglycines
Requirement of N-substitution	N-substituents are required for substrate stability/reactivity	No preinstalled N-substituents, nitrogen introduced as NH_2OH from NO_2^-, enabling formation of free NH_2 groups
Nitrogen source	Already in the organic substrate (no NO_x^{y-} valorization)	NO_2^-, extendable to NO_3^-/NO
Post-synthesis treatment	Additional deprotection or transformation steps are required to access free amino acids	Direct access to free amino acids, avoiding extra post-treatment steps
Imine reactants/intermediates	Imines with stabilizing N-substituents as reactants	Imine intermediates generated in situ from oxime reduction

Supplementary Table 3. Raman peaks identified in Fig. S20 and their assignment to PhGly.

Raman wavenumber (cm^{-1})	**Assignment**
3059	NH_3^+ asymmetric stretching
2979	φ CH stretching
1608~1540	Quadrant ring stretching
1409.5~1388	Fermi resonance
1359	CH chain deformation
1297	φ sextant ring stretching; OH in-plane deformation
1202	φ ring–C stretching; C–O(H) stretching; in-plane CH deformation
1003.5	φ ring breathing; φ in-plane ring deformation
903	α-C–C(OOH) skeletal stretching
858	C–C–N symmetric stretching
780	in-phase out-of-plane CH (ring) wagging
735	φ out-of-plane CH deformation
687	φ out-of-plane sextant ring deformation
513	C–C=O in-plane deformation